

Stripes, Zigzags, and Slow Dynamics in Buckled Hard Spheres

Yair Shokef* and Tom C. Lubensky

Department of Physics and Astronomy, University of Pennsylvania, Philadelphia, PA 19104, USA

(Dated: December 18, 2008)

We study the analogy between buckled colloidal monolayers and the triangular-lattice Ising anti-ferromagnet. We calculate free volume-induced Ising interactions, show how lattice deformations favor zigzag stripes that partially remove the Ising model ground-state degeneracy, and identify the Martensitic mechanism prohibiting perfect stripes. Slowly inflating the spheres yields jamming as well as logarithmically slow relaxation reminiscent of the glassy dynamics observed experimentally.

PACS numbers: 82.70.Dd, 75.50.Ee, 75.10.Hk, 81.30.Kf

Geometric frustration, manifested for example in the anti-ferromagnetic (AF) Ising model on a triangular lattice [1], occurs whenever local interaction energies cannot be simultaneously minimized. It gives rise to highly degenerate ground states, unusual phases of matter [2], and possibly slow or glassy dynamics [3], whose properties even after decades of research are not fully understood. Here we present a theoretical study of a colloidal system, one of a class of artificial frustrated systems in which the state of each constituent can be directly visualized [4], that provides new insight into the microstructure of frustrated systems and its connection with their dynamics.

We study hard spheres confined between parallel plates. For plate separation slightly greater than the sphere diameter and at sufficiently high sphere density, the spheres buckle upward or downward [5, 6, 7] from their lower-density positions on a hexagonal lattice. This buckling gives rise to a choice of two states for each sphere, analogous to the two states of Ising-model spins [5, 8]. The tendency of spheres to maximize free volume introduces an effective repulsive interaction that favors configurations with neighboring spheres in opposite states just as the AF Ising interaction favors opposite states of neighboring spins. As in the triangular-lattice AF Ising model, frustration arises because it is impossible to arrange the three particles on any triangular plaquette such that all pairs of neighboring particles are in opposite states. In the AF Ising model on a rigid lattice, there is an extensive number of ground-state configurations (implying an extensive ground-state entropy) in which neighboring spins on two of the three bonds on each plaquette are in opposite states. Given the analogy just drawn between our colloidal system and the AF Ising model, it is reasonable to conjecture that the colloidal system might exhibit ground-state degeneracies and dynamics similar to those of the rigid-lattice AF Ising model. Recent experiments in diameter-tunable-microgel systems revealed sub-extensive ground-state entropy and glassy dynamics [9]. Our theoretical study will address the differences between the colloidal system and the rigid lattice Ising model and make some conjectures about a likely closer analogy between the colloidal system and the AF Ising model on a compressible lattice [10].

We show that the short-ranged AF behavior in this hard-sphere system may be explained by a simple geometrical model relating it to the nearest-neighbor Ising model. However, the out-of-plane buckling induces local in-plane lattice distortions that, as in the elastic Ising model, partially remove the Ising ground-state degeneracy and select configurations with zigzagging stripes of up and down spheres. This ‘ground-state’ lacks the local zero-energy modes found in the Ising model on a rigid triangular lattice, and as a result, the colloidal system exhibits dynamics that are qualitatively slower than those of the Ising model. Moreover, stripes require global deformations that are incompatible with the system’s boundary conditions; consequently they break up into a Martensite [11] and form a new partially disordered and highly degenerate ‘ground-state’.

The free energy of our hard-sphere system is dictated by its phase-space volume, which is a collective function of all the particles in the system; hence this system is not exactly equivalent to an Ising model with pairwise additive interactions. Nonetheless, we may compare our system to the nearest-neighbor Ising model on the triangular lattice and ask what is the strength of AF interactions that best describes the hard-sphere system.

A ‘microscopic’ state is specified by the positions $\{x_i, y_i, z_i\}$ of all particles $1 \leq i \leq N$. We coarse-grain these states into Ising-like configurations specified by $\{s_i\}$ with $s_i = \text{sign}(z_i)$ (x, y are the coordinates in the plane of the confining walls, z is perpendicular to the walls, and $z = 0$ is at the middle of the cell). The probability of a particular configuration $\{s_i\}$ is equal to the $3N$ -dimensional integral $V(\{s_i\})$ over all states belonging to that configuration, divided by the total phase-space volume V_{tot} of all configurations:

$$P_{\text{HS}}(\{s_i\}) = V(\{s_i\}) / V_{\text{tot}}. \quad (1)$$

We would like to equate this to the probability of finding the corresponding configuration in the Ising model,

$$P_{\text{I}}(\{s_i\}) = \exp\left(\beta J \sum s_i s_j\right) / Z, \quad (2)$$

where $\beta = 1/k_B T$ is the inverse temperature, J is the interaction strength, the sum runs over all nearest neighbor pairs, and Z is the canonical partition function.

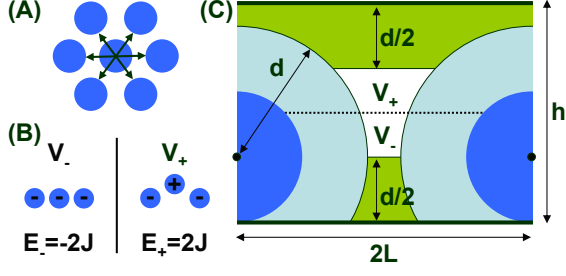


FIG. 1: (Color online) Free volume model: A) Top view. Contributions to free volume originate from motion along axes to each of the neighbors. B) Side view. Up particle surrounded by down particles has more free volume (lower energy) than a down particle. C) Surrounding neighbors touch wall and are separated by $2L$, central particle is confined to the vertical plane. Large circles are volumes excluded by neighbors, horizontal bands are volumes excluded by the walls, remaining white region is the central particle's free volume, divided at the middle of the cell height (dotted line) into V_+ and V_- .

Unlike the commonly used cell-model, which approximates the phase-space volume of a system as a product of single-particle free volumes, our model equates P_{HS} and P_I by assuming that $V(\{s_i\})$ is a product of contributions from all nearest-neighbor ‘bonds’: $V(\{s_i\}) = \prod v(s_i s_j; h, d, L)$, where the pair contribution v depends on $s_i s_j$ and on the wall separation h , the sphere diameter d , and the in-plane number density, which we characterize by the spacing L of the underlying triangular lattice. We evaluate $v(s_i s_j)$ in a quasi-one-dimensional approximation by allowing particles i and j to move only in the vertical plane passing through the axis connecting their lattice positions (see Fig. 1A). We consider a particle, which we call the central particle, and its two neighbors along one of the principal lattice directions (see Fig. 1B). If the two neighbors are in opposite Ising states, the free volumes resulting from the central one being up or down are equal by symmetry. When the two neighbors are in the same state (down, without loss of generality), the central particle has more free volume (V_+) when it is up than when it is down (V_-). We calculate V_+ and V_- from the geometrical setting of Fig. 1C and equate the ratio of the probabilities of finding the two configurations in Fig. 1B for hard spheres to that of the Ising model:

$$\frac{V_+}{V_-} = \frac{\exp(-\beta E_+)}{\exp(-\beta E_-)} = \exp(-4\beta J). \quad (3)$$

From this, we deduce that the hard-sphere system corresponds to an Ising model with an effective AF interaction, $\beta J_{\text{eff}}(d, h, L) = -\ln(V_+/V_-)/4 < 0$.

For given geometrical parameters d , h , L , we evaluate V_+ and V_- and determine the effective interaction strength βJ_{eff} . We then use the exact solution of the Ising model [1] to calculate the average number $\langle N_f \rangle$ of frustrated neighbors per particle (we refer to $s_i s_j = -1$ as satisfied and to $s_i s_j = 1$ as frustrated), which pro-

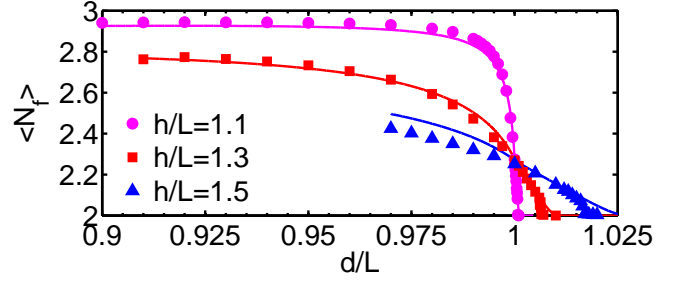


FIG. 2: (Color online) Average number of frustrated bonds per particle vs sphere diameter and cell height. Free-volume model (lines) agrees with Monte-Carlo simulations (symbols).

vides a measure of short-range AF order. $\langle N_f \rangle = 2$ is the value in the ground state, and $\langle N_f \rangle = 3$ corresponds to a random configuration. Figure 2 shows the agreement between our simple model and three-dimensional Monte-Carlo (MC) simulations. Simulations included $N = 1600$ spheres with steps consisting of small displacements of single spheres as well as area-preserving box deformations, in which the angle or aspect ratio of the simulated parallelogram was allowed to change [7]. To probe cases with $d > L$, we start with striped configurations that can accommodate the maximal sphere diameter by lattice deformation (see below), wait 4×10^5 steps, and then average $\langle N_f \rangle$ over additional 4×10^5 steps. We plot results only of cases for which d was large enough for the system to have long-range six-fold orientational order $\Psi_6 \equiv \langle \exp(i6\theta_{jk}) \rangle > 0.5$ (θ_{jk} is the angle the bond between j and k forms with an arbitrary axis, and the average is over all nearest-neighbors pairs [12]). Small spheres ($d < L$) in a wide cell ($h/L = 1.5$) are weakly confined, and the approximation that the surrounding spheres in Fig. 1C touch the walls fails, giving rise to small differences between the model and simulations.

For large spheres ($d > L$), simulations remain jammed in striped configurations and do not increase the value of $\langle N_f \rangle$ beyond the initial value of 2, even though they are expected to do so from the free volume considerations incorporated in the model. To further explore this jamming, we conducted MC simulations that started at a disordered configuration with $d_0 = L$ and then ordered as the sphere diameter was gradually increased to some larger value d . The spheres were initially on a triangular lattice in the xy plane with each sphere randomly touching either the top or bottom wall. To speed the simulations, we considered random jumps in the z direction between touching either walls, while keeping the xy displacements continuous. During the swelling process, once every MC step the diameter of all spheres was increased to the maximal value allowable without overlaps. Figure 3 shows results of simulations with wall separation $h/L = 1.3$. For $d/L = 1.005$, the free-volume model predicts $\langle N_f \rangle = 2.12$, and the simulation indeed slowly equilibrates to that value by $\sim 10^5$ MC steps. For $d/L = 1.01$,

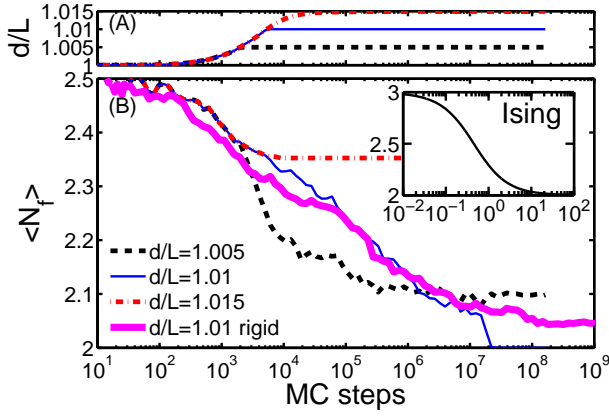


FIG. 3: (Color online) A) Sphere diameter, and, B) average number of frustrated bonds per particles following swelling to different sphere diameters. Normalized cell height $h/L = 1.3$. Inset: same for Ising model following quench to $T = 0$.

the system's relaxation to the value of $\langle N_f \rangle = 2$ predicted by the model includes a logarithmically slow decay to $\langle N_f \rangle \approx 2.1$ over a time scale of 10^7 MC steps, followed by a sharp jump to the equilibrium state. For $d/L = 1.015$, although the system is expected to be at a state with $\langle N_f \rangle = 2$, it gets jammed during the swelling process at a state with $\langle N_f \rangle = 2.35$ and does not leave it over the time scales investigated here. Note that in Fig. 3 we plot a single realization for each case, however we observed similar behavior when repeating the simulations with multiple realizations. Neither jamming nor logarithmically slow relaxation occur in the Ising model even when quenched to zero temperature (see inset).

Densely-packed spheres exhibit slower dynamics than low-temperature Ising spins on a rigid lattice because the morphology of the maximally-packed hard-sphere configurations differ from those of the Ising ground-state. Unlike the highly disordered Ising ground-state [1], the hard-sphere 'ground-state' consists of parallel zigzag stripes (Fig. 4A). In the Ising model, each triangular plaquette has one bond frustrated and two satisfied. Although one third of the bonds in the system are frustrated, and the average number of frustrated neighbors per particle is $\langle N_f \rangle = 2$, not all particles have exactly two frustrated neighbors. By considering the six triangles surrounding a certain spin in the lattice, Fig. 5A shows the five possible ways (up to rotations and spin inversions) to align them such that each triangle will have a single frustrated bond. The central spin may have $N_f = 0, 1, 2$, or 3 frustrated neighbors. This leads not only to disorder but also to fast relaxation dynamics since spins with $N_f = 3$ are free to flip without an energetic cost. For close-packed buckled spheres, each triplet of spheres in contact defines an equilateral triangle with sides d . As in the Ising model, one of the three spheres is up (or down) and two down (or up), thus tilting this equilateral triangle with respect to the horizontal plane. When projected onto the plane,

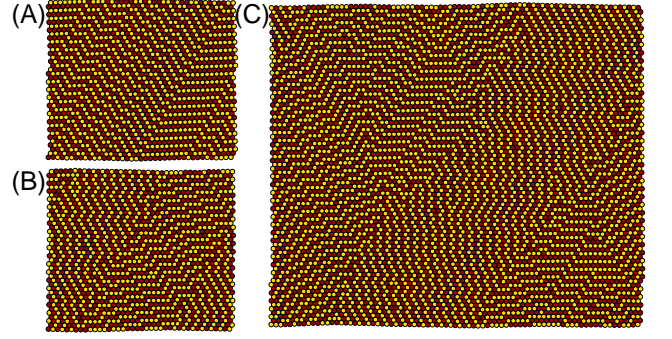


FIG. 4: (Color online) Final configurations following swelling to $d/L = 1.01$ at $h/L = 1.3$. A) Deformable box. B-C) Rigid box. System has $N = 1600$ (A-B), 6400 (C) spheres. Spheres touching top/bottom wall are dark/bright. Simulation boxes are deformed parallelograms with periodic boundary conditions. For ease of presentation we copy the simulated region and plot a rectangular region of the periodic system.

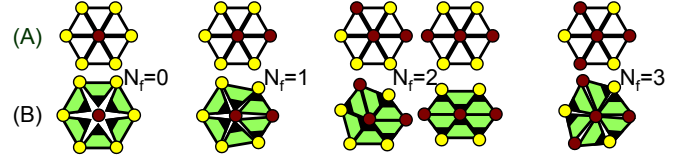


FIG. 5: (Color online) Tiling with: A) equilateral triangles for the Ising ground-state, and, B) isosceles triangles for close-packed buckled hard spheres. The large angle β is blackened.

the tilted equilateral triangle is deformed to an isosceles triangle with one long side d along the frustrated bond and two shorter sides $x = \sqrt{d^2 - (h-d)^2} < d$ along the satisfied bonds. Each of these isosceles triangles has two small angles $\alpha = \cos^{-1}(\frac{d}{2x}) < \frac{\pi}{3}$ and a large angle $\beta = \pi - 2\alpha > \frac{\pi}{3}$. Now, close-packed configurations for the buckled spheres are equivalent to tiling the plane with these isosceles triangles. To completely cover the plane, the angles of the six triangles meeting at each vertex must sum to 2π . Figure 5B demonstrates that for $N_f = 0, 1, 3$ the angles sum to $6\beta > 2\pi$, $2\alpha + 4\beta > 2\pi$, and $6\alpha < 2\pi$, respectively, and thus that the triangles cannot fit together: for the two configurations with $N_f = 2$ the angles sum to $4\alpha + 2\beta = 2\pi$, enabling a perfect tiling corresponding to the maximal-density close-packed state.

The slow dynamics observed for large sphere diameters result from the lower degeneracy of these zigzagged stripe configurations compared to the Ising ground-state. More importantly, the close-packed states with $N_f \equiv 2$ do not have the free particles with $N_f = 3$ that are crucial for the low-temperature dynamics in the Ising model [13]. Here, many spheres need to cooperatively rearrange in order for the system to find configurations that maximize the free volume. Spheres swollen to a very large diameter ($d/L = 1.015$ here) hardly move vertically to change their Ising-configuration because the neighboring spheres do not have enough room to rearrange in the horizontal

directions and to accommodate the lattice deformations required to achieve optimal packing.

When the spheres swell slowly enough, they find a configuration that maximizes free-volume by each sphere having exactly two frustrated neighbors. Such configurations consist of parallel zigzagging stripes (Fig. 4A). Stripes run only along two of the three principal lattice directions, hence the local distortions are non-isotropic and require a macroscopic deformation of the system. This is possible in the simulations described above in which the shape of the simulation's bounding-box changes dynamically [7]. However, experimentally the spheres form crystalline domains separated by grain boundaries [12], which may be better described theoretically by rigid boundary conditions. Then, the local tendency for zigzag stripes is incompatible with the rigid boundary conditions. The tiling rules for the isosceles triangles induce local deformations along two of the three principal lattice directions, and for the system to be globally isotropic it must break up into domains with stripes running along different directions. We suspect that this is the mechanism leading to the broken stripes seen experimentally [9] and we indeed observed such Martensitic states [11] when repeating the swelling simulations without allowing the simulation box to deform [14]. For instance, the case of $h/L = 1.3$, $d/L = 1.01$ relaxes in the deformable box simulations to the zigzagged striped state with $N_f \equiv 2$, whereas in a rigid box, the average number of frustrated neighbors relaxes to $\langle N_f \rangle = 2.05$ (Fig. 3B), and the final configuration (Fig. 4B) consists of broken stripes. We saw similar structures (Fig. 4C) and relaxation to the same value of $\langle N_f \rangle$ for $N = 100, 400, 1600, 6400$. It would be interesting to test whether the size of these domains scales as the square root of the system size, as was found in other Martensites [11], and whether subsequently $\langle N_f \rangle$ slowly goes to 2 in the large- N limit.

The maximal sphere diameter possible in a zigzag configuration is equal to that of straight stripes, and the free-volume-cell approximation does not distinguish between the two $N_f = 2$ configurations corresponding to a straight segment of a stripe and to a bend in the stripes. However simulations and experiments seem to indicate a possible preference for straight stripes over zigzags. It is unclear if the observed zigzag patterns represent equivalence between straight and zigzagged stripes, or whether the system falls into zigzagged configurations due to kinetic reasons. It would be interesting to go beyond the mean-field description, as was done when comparing the face-centred cubic and the random hexagonal-close-packed structure of hard spheres in three dimensions [15].

The relief of frustration by lattice deformation resembles the elastic Ising model [10], which when analyzed exactly at the microscopic level yields by our isosceles tiling scheme a zigzag-stripe ground-state. It would be interesting to further investigate the finite temperature behavior

of that model, as well as other models with zigzag-stripe ground-states [16].

We thank Yilong Han, Matt Lohr, Arjun Yodh, and Peter Yunker for involving us in their experimental study of this topic, and Bulbul Chakraborty, Randy Kamien, Andrea Liu, Carl Modes, Yehuda Snir, and Anton Souslov for helpful discussions. This work is supported by NSF MRSEC grant DMR-0520020.

* Present Address: Physics of Complex Systems, Weizmann Institute of Science, Rehovot 76100, Israel.

- [1] G.H. Wannier, Phys. Rev. **79**, 357 (1950); Phys. Rev. B **7**, 5017 (1973). R.M.F. Houtappel, Physica **16**, 391 (1950); Physica **16**, 425 (1950).
- [2] R. Moessner and A.R. Ramirez, Phys. Today **59**, 24 (2006).
- [3] G. Tarjus, S. A. Kivelson, Z. Nussinov, and P. Viot, J. Phys.: Condens. Matter **17** R1143 (2005).
- [4] D. Davidović *et al.*, Phys. Rev. Lett. **76**, 815 (1996); Phys. Rev. B **55**, 6518 (1997). H. Hilgenkamp *et al.*, Nature **422**, 50 (2003). R.F. Wang *et al.*, Nature **439**, 303 (2006). Y. Qi, T. Brintlinger, and J. Cumings, Phys. Rev. B **77**, 094418 (2008). A. Libál, C. Reichhardt, and C.J. Olson Reichhardt, Phys. Rev. Lett. **97**, 228302 (2006).
- [5] P. Pieranski, L. Strzelecki, and B. Pansu, Phys. Rev. Lett. **50**, 900 (1983).
- [6] B. Pansu, Pi. Pieranski, and Pa. Pieranski, J. Physique **45**, 331 (1984). D.H. Van Winkle and C.A. Murray, Phys. Rev. A **34**, 562 (1986). T. Chou and D.R. Nelson, Phys. Rev. E **48**, 4611 (1993). P. Melby *et al.*, J. Phys. Cond. Mat. **17**, S2689 (2005). N. Osterman, D. Babič, I. Poberaj, J. Dobnikar, and P. Zihlerl, Phys. Rev. Lett. **99**, 248301 (2007).
- [7] M. Schmidt and H. Löwen, Phys. Rev. Lett. **76**, 4552 (1996); Phys. Rev. E **55**, 7228 (1997). R. Zangi and S.A. Rice, Phys. Rev. E **58**, 7529 (1998); **61**, 660 (2000).
- [8] T. Ogawa, J. Phys. Soc. Jpn. Suppl. **52**, 167 (1983).
- [9] Y. Han *et al.*, Nature **456**, 898 (2008).
- [10] Z.Y. Chen and M. Kardar, J. Phys. C: Solid State Phys. **19**, 6825 (1986). L. Gu, B. Chakraborty, P.L. Garrido, M. Phani, and J.L. Lebowitz, Phys. Rev. B **53**, 11985 (1996).
- [11] K. Bhattacharya, *Microstructure of Matersite* (Oxford University Press, New-York, 2003).
- [12] Y. Han, N.Y. Ha, A.M. Alsayed, and A.G. Yodh, Phys. Rev. E **77** 041406 (2008).
- [13] E. Kim, B. Kim, and S.J. Lee, Phys. Rev. E **68**, 066127 (2003).
- [14] Note that this equilateral-to-isosceles deformation differs from the square-to-triangle Martensitic transition studied in: J.A. Weiss, D.W. Oxtoby, D.G. Grier, and C.A. Murray, J. Chem. Phys. **103**, 1180 (1995).
- [15] W.G. Rudd, Z.W. Salsburg, A.P. Yu, and F.H. Stillinger, J. Chem. Phys. **49**, 4857 (1968). P.N. Pusey *et al.*, Phys. Rev. Lett. **63**, 2753 (1989). S.C. Mau and D.A. Huse, Phys. Rev. E **59**, 4396 (1999). C. Radin and L. Sadun, Phys. Rev. Lett. **94**, 015502 (2005). H. Koch, C. Radin, and L. Sadun, Phys. Rev. E **72**, 016708 (2005).
- [16] Z. Nussinov, Phys. Rev. B **69**, 014208 (2004).